

Visualizing quantum mechanics in phase space

Heiko Bauke^{a)} and Noya Ruth Itzhak

Max-Planck-Institut für Kernphysik, Saupfercheckweg 1, 69117 Heidelberg, Germany

(Dated: 26 November 2024)

We examine the visualization of quantum mechanics in phase space by means of the Wigner function and the Wigner function flow as a complementary approach to illustrating quantum mechanics in configuration space by wave functions. The Wigner function formalism resembles the mathematical language of classical mechanics of non-interacting particles. Thus, it allows a more direct comparison between classical and quantum dynamical features.

PACS numbers: 03.65.-w, 03.65.Ca

Keywords:

1. Introduction

Quantum mechanics is a corner stone of modern physics and technology. Virtually all processes that take place on an atomar scale require a quantum mechanical description. For example, it is not possible to understand chemical reactions or the characteristics of solid states without a sound knowledge of quantum mechanics. Quantum mechanical effects are utilized in many technical devices ranging from transistors and Flash memory to tunneling microscopes and quantum cryptography, just to mention a few applications.

Quantum effects, however, are not directly accessible to human senses, the mathematical formulations of quantum mechanics are abstract and its implications are often unintuitive in terms of classical physics. This poses a major challenge in teaching and learning the foundations of quantum mechanics and makes it difficult for students to form a mental picture of quantum dynamical processes. Therefore, teaching quantum mechanics may be supported by visualizing the mathematical objects of quantum mechanics' mathematical language in order to sharpen the students' understanding of abstract concepts. In fact, many text books¹⁻⁴ communicate quantum mechanics with the aid of visual means.

Visualizing quantum dynamics is typically implemented by providing a pictorial representation of the quantum mechanical wave function in position space⁵ or in momentum space⁶. In order to establish a relation between quantum dynamics and classical dynamics, the phase space seems to be more appropriate because classical Hamiltonian mechanics is formulated in phase space. Thus, we will present in this contribution methods to visualize quantum dynamics in phase space.

The remainder of this paper is organized as follows. In section 2 we briefly review how to depict quantum dynamics in position space or in momentum space using wave functions. In section 3 we give a short introduction to quantum mechanics in phase space and establish some connections between quantum mechanics and many-particle classical mechanics before we visualize quantum dynamics in phase space in section 4.

2. Visualizing quantum dynamics in position space or momentum space

A (one-dimensional) quantum mechanical position space wave function maps each point x on the position axis to a time dependent complex number $\Psi(x, t)$. Equivalently, one may consider the wave function $\tilde{\Psi}(p, t)$ in momentum space, which is given by a Fourier transform of $\Psi(x, t)$, viz.

$$\tilde{\Psi}(p, t) = \frac{1}{(2\pi\hbar)^{1/2}} \int \Psi(x, t) e^{-ixp/\hbar} dx. \quad (1)$$

Various methods to visualize complex-valued functions in position space or momentum space have been devised. Figure 1 exemplifies three different ways of visualizing a wave function. It shows a Gaussian wave packet

$$\Psi(x, t) = \frac{1}{\left(2\pi\sigma^2 \left(1 + \frac{i\hbar t}{2m\sigma^2}\right)^2\right)^{1/4}} \exp\left(\left(-\frac{(x - \bar{x})^2}{4\sigma^2} + \frac{i\bar{p}(x - \bar{x})}{\hbar} - \frac{i\bar{p}^2 t}{2m\hbar}\right)\right) \left(1 + \frac{i\hbar t}{2m\sigma^2}\right) \quad (2)$$

in position space with mass m , mean position \bar{x} , mean momentum \bar{p} , and width σ at time $t = 0$.

Part a of Fig. 1 presents the complex wave function (2) by plotting its real and its imaginary part as separate real-valued functions. Although a complex function is completely determined by specifying its real and its imaginary part it is difficult to infer physically relevant information from these separated quantities.

Visualizing the wave-function's squared modulus and its phase is more appropriate because the squared modulus of a wave function may be interpreted as a probability distribution and the change of its phase encodes information about the momentum. Thus, we picture the wave function (2) in part b of Fig. 1 by small directional arrows. Each arrow's length is determined by the wave-function's modulus, its direction (angle between the arrow and the horizontal axis) by the wave-function's phase. The arrows in Fig. 1 b are sometimes called phasors. The method to portray a wave function by phasors

^{a)}Electronic mail: bauke@mpi-hd.mpg.de

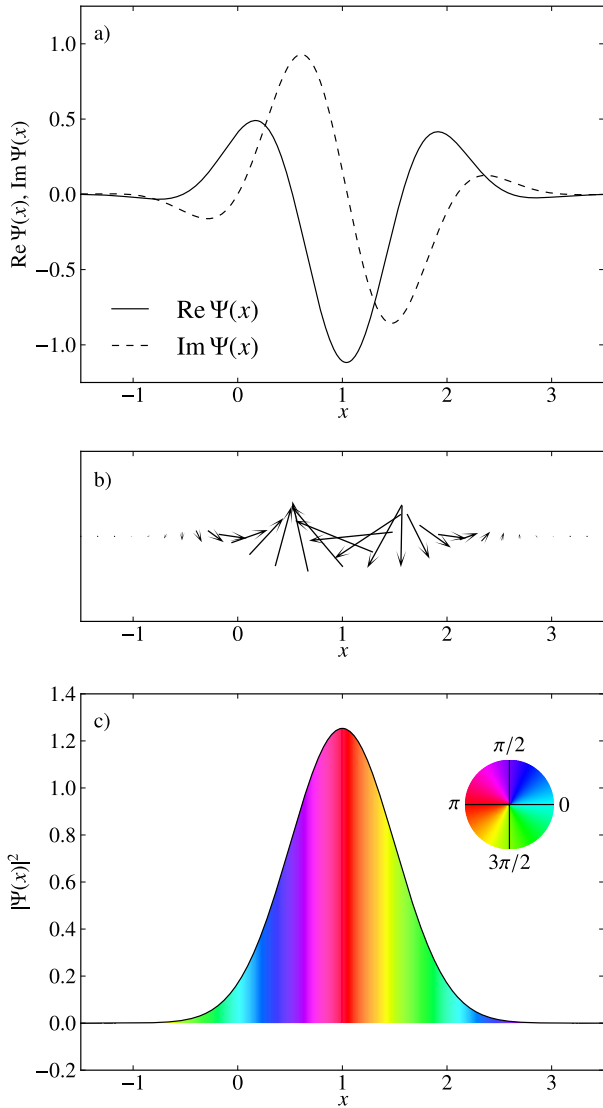


FIG. 1: (Color online) Three different ways of visualizing the Gaussian wave packet (2) at time $t = 0$ with $\bar{x} = 1$, $\bar{p} = 3$, and $\sigma = 1/2$ (dimensionless units with $\hbar = 1$ and $m = 1$); a) visualization by the wave-function's real part and imaginary part, b) visualization by the wave-function's modulus and its phase using arrows (phasors), c) visualization by plotting the wave-function's squared modulus and encoding the phase in a periodic color scheme.

had been used, for example, by Feynman⁷. It is beneficial in situations where advanced printing methods, color printing for example, are not available. However, it is difficult to picture fast oscillatory wave functions in this manner.

Another way of presenting a wave function by its modulus and its phase has been popularized by Thaller^{1,2}. This method is utilized in part c of Fig. 1. It shows the squared modulus of the wave function (2) plus its phase which is encoded by the color between the graph of the squared modulus and the horizontal axis. Plotting the squared modulus allows for a direct read off of the probability distribution in position space. Note that the color scheme for the phase in part c of

Fig. 1 is 2π -periodic and contiguous. Encoding the phase as a color allows to plot even relatively strongly oscillating wave functions. It requires, however, high-quality color printing for good reproduction. Thaller^{1,2} has also generalized this approach to multi-component wave functions.

3. Quantum mechanics in phase space

3.1. The Wigner function

The Wigner distribution function⁸⁻¹⁰ was introduced by Eugene Paul Wigner to take into account quantum corrections to classical statistical mechanics in 1932. Today, it finds applications in current research in various branches of physics ranging from quantum optics¹¹ and quantum chaos¹² to nuclear and solid state physics. The Wigner function allows for a mathematical description of (non-relativistic) quantum mechanics in phase space. But it is more than a sheer mathematical object, it may be reconstructed by a series of measurements¹³⁻¹⁷. The Wigner function formalism is mathematically equivalent to the standard language of quantum mechanics in terms of wave functions and the Schrödinger equation but it is more closely related to classical mechanics because it formulates quantum mechanics in phase space as Hamiltonian mechanics does.

The Wigner function of a (one-dimensional) pure state wave function $\Psi(x, t)$ is defined as

$$w(x, p, t) = \frac{1}{2\pi\hbar} \int \Psi^*(x + s/2, t) \Psi(x - s/2, t) e^{isp/\hbar} ds, \quad (3)$$

where $\Psi^*(x, t)$ denotes the complex conjugate of $\Psi(x, t)$. Note that due to the symmetry of the integrand in (3), the Wigner function $w(x, p, t)$ is always a real function. The expression

$$w(x, p, t) = \frac{1}{2\pi\hbar} \int \tilde{\Psi}^*(p + s/2, t) \tilde{\Psi}(p - s/2, t) e^{-isx/\hbar} ds \quad (4)$$

is equivalent to (3) if $\Psi(x, t)$ and $\tilde{\Psi}(p, t)$ are linked via (1). Further important mathematical properties^{9,11} of the Wigner function include the following relations.

- If $\Psi(x, t)$ is normalized to one then also $w(x, p, t)$, viz.

$$\iint w(x, p, t) dp dx = 1, \quad (5)$$

furthermore, the equation

$$\iint w(x, p, t)^2 dp dx = \frac{1}{2\pi\hbar} \quad (6)$$

holds for all pure states $\Psi(x, t)$.

- Quantum mechanical probability densities in position space and momentum space may be obtained from the marginals of the Wigner function

$$\rho(x, t) = |\Psi(x, t)|^2 = \int w(x, p, t) dp, \quad (7a)$$

$$\rho(p, t) = |\tilde{\Psi}(p, t)|^2 = \int w(x, p, t) dx. \quad (7b)$$

- The state overlap of two wave functions $\Psi_1(x, t)$ and $\Psi_2(x, t)$ in terms of their Wigner functions $w_1(x, p, t)$ and $w_2(x, p, t)$ reads

$$\int \Psi_1^*(x, t) \Psi_2(x, t) dx = 2\pi\hbar \iint w_1(x, p, t) w_2(x, p, t) dp dx. \quad (8)$$

- The Wigner function obeys the reflection symmetries

$$\Psi(x, t) \rightarrow \Psi^*(x, t) \Rightarrow w(x, p, t) \rightarrow w(x, -p, t), \quad (9)$$

$$\Psi(x, t) \rightarrow \Psi(-x, t) \Rightarrow w(x, p, t) \rightarrow w(-x, -p, t). \quad (10)$$

- The Wigner function is Galilei-covariant, that is

$$\Psi(x, p, t) \rightarrow \Psi(x + y, p, t) \Rightarrow w(x, p, t) \rightarrow w(x + y, p, t), \quad (11)$$

but not Lorentz-covariant. However, Lorentz-covariant generalizations of the Wigner function have been considered in the literature^{18–20} which may be applied in relativistic quantum optics²¹.

- The Wigner function is not gauge invariant. The definition (3), however, may be generalized²² such that it becomes independent of the gauge in the presence of a magnetic field.

The Wigner function $w(x, p, t)$ is called *quasi* probability function because it is real and normalized to one but not strictly non-negative. In fact, a sufficient and necessary condition that $w(x, p, t)$ is strictly non-negative is that $\Psi(x, t)$ is a minimum uncertainty wave packet, that is a Gaussian wave packet²³. As a consequence of (6), the Wigner function can not be arbitrarily highly peaked, which is a reminiscence of the quantum mechanical uncertainty relation.

The evolution equation^{9,11,24,25} of the Wigner function may be obtained by calculating the Wigner-function's time derivative. Taking into account the Schrödinger equation

$$i\hbar \frac{\partial \Psi(x, t)}{\partial t} = \hat{H} \Psi(x, t) = -\frac{\hbar^2}{2m} \frac{\partial^2 \Psi(x, t)}{\partial x^2} + V(x, t) \Psi(x, t) \quad (12)$$

for the wave function moving in the potential $V(x, t)$ we get

$$i\hbar \frac{\partial w(x, p, t)}{\partial t} = \frac{1}{2\pi\hbar} \int ((\hat{H} \Psi(x, t)) \Psi(x, t)^* - \Psi(x, t) (\hat{H} \Psi(x, t))^*) e^{isp/\hbar} ds. \quad (13)$$

After several algebraic manipulations that include expanding the potential $V(x, t)$ into a Taylor series around $x = 0$ and integrating (13) by parts one finally finds the so-called quantum Liouville equation

$$\frac{\partial w(x, p, t)}{\partial t} = \sum_{l=0}^{\infty} \frac{(i\hbar/2)^{2l}}{(2l+1)!} \left(\frac{\partial}{\partial p_w} \frac{\partial}{\partial x_H} - \frac{\partial}{\partial p_H} \frac{\partial}{\partial x_w} \right)^{2l+1} H(x, p, t) w(x, p, t), \quad (14)$$

which is a partial differential equation of infinite degree. The operator $\left(\frac{\partial}{\partial x_w} \frac{\partial}{\partial p_H} - \frac{\partial}{\partial p_H} \frac{\partial}{\partial x_w} \right)$ in (14) consists of differential operators that act on the Hamilton function $H(x, p, t)$ (indicated by the index H) and differential operators that act on the Wigner function $w(x, p, t)$ (indicated by the index w). The function $H(x, p, t)$ in (14) is the classical Hamilton function

$$H(x, p, t) = \frac{p^2}{2m} + V(x, t) \quad (15)$$

that corresponds to the Hamilton operator \hat{H} of the Schrödinger equation (12).

For systems where magnetic fields are absent as in (12), the Hamilton function $H(x, p, t)$ can be written as a sum of a kinetic energy term $K(p) = p^2/(2m)$ that depends only on the momentum p and a potential energy term $V(x, t)$ that depends only on the position x (and possibly the time t). In this case, the quantum Liouville equation (14) may be written as a continuity equation

$$\frac{\partial w(x, p, t)}{\partial t} = - \left(\frac{\partial}{\partial p} \right) \cdot \mathbf{j}(x, p, t), \quad (16)$$

where we have introduced the two-dimensional vector field

$$\mathbf{j}(x, p, t) = \left(\begin{array}{c} \frac{p}{m} w(x, p, t) \\ - \sum_{l=0}^{\infty} \frac{(i\hbar/2)^{2l}}{(2l+1)!} \left(\frac{\partial}{\partial p} \frac{\partial}{\partial x_v} - \frac{\partial}{\partial x_w} \right)^{2l} \frac{\partial V(x, t)}{\partial x} w(x, p, t) \end{array} \right), \quad (17)$$

called the Wigner function flow.

Let \hat{O}_x denote some operator function of the quantum mechanical position operator and $O(x)$ the corresponding classical function, then it follows from (7b) that

$$\langle O_x \rangle(t) = \langle \Psi(x, t) | \hat{O}_x | \Psi(x, t) \rangle = \iint w(x, p, t) O(x) dp dx. \quad (18)$$

This means one can calculate the quantum mechanical expectation value $\langle O_x \rangle(t)$ of an operator \hat{O}_x by averaging the classical function $O(x)$ over the Wigner function $w(x, p, t)$. For momentum dependent operators \hat{O}_p and their corresponding classical functions one finds using (7a) a similar statement

$$\langle O_p \rangle(t) = \langle \Psi(x, t) | \hat{O}_p | \Psi(x, t) \rangle = \iint w(x, p, t) O(p) dp dx. \quad (19)$$

For general operators $\hat{O}_{x,p}$ and classical functions $O(x, p)$ that depend on the position as well as on the momentum one can show^{9,24} that

$$\langle O_{x,p} \rangle (t) = \langle \Psi(x, t) | \hat{O}_{x,p} | \Psi(x, t) \rangle = \iint w(x, p, t) O(x, p) dp dx \quad (20)$$

provided that the relation between the operator $\hat{O}_{x,p}$ and the function $O(x, p)$ is established by

$$\hat{O}_{x,p} = \iint \tilde{O}(\xi, \pi) e^{i(\xi\hat{x} + \pi\hat{p})/\hbar} d\xi d\pi, \quad (21)$$

where $\tilde{O}(\xi, \pi)$ denotes the Fourier transform of $O(x, p)$

$$\tilde{O}(\xi, \pi) = \iint O(x, p) e^{-i(x\xi + p\pi)/\hbar} dx dp \quad (22)$$

and \hat{x} the position operator and \hat{p} the canonical momentum operator, respectively.

The Wigner function $w_E(x, p)$ of an energy eigen-state wave function of the Hamiltonian $H(x, p) = p^2/(2m) + V(x)$ is time independent and therefore it follows from (14) that

$$\left(\frac{p}{m} \frac{\partial}{\partial x} - \sum_{l=0}^{\infty} \frac{(i\hbar/2)^{2l}}{(2l+1)!} \frac{\partial^{2l+1} V(x)}{\partial x^{2l+1}} \frac{\partial^{2l+1}}{\partial p^{2l+1}} \right) w_E(x, p) = 0. \quad (23a)$$

This equation, however, is not sufficient to specify the energy eigen-value E , which is determined by the eigen-value equation¹¹

$$\left(\frac{p^2}{2m} - \frac{\hbar^2}{8m} \frac{\partial^2}{\partial x^2} + \sum_{l=0}^{\infty} \frac{(i\hbar/2)^{2l}}{(2l)!} \frac{\partial^{2l} V(x)}{\partial x^{2l}} \frac{\partial^{2l}}{\partial p^{2l}} \right) w_E(x, p) = E w_E(x, p). \quad (23b)$$

The two equations (23a) and (23b) together are equivalent to the time independent Schrödinger eigen-value equation

$$-\frac{\hbar^2}{2m} \frac{\partial^2 \Psi_E(x, t)}{\partial x^2} + V(x, t) \Psi_E(x, t) = E \Psi_E(x, t). \quad (24)$$

3.2. Relations to classical mechanics

The motion of an ensemble of classical non-interacting particles may be characterized by a probability distribution $w(x, p, t)$ in phase space.²⁶ The probability distribution $w(x, p, t)$ determines how likely it is that a particle in the ensemble is at position x and has momentum p at time t . It allows to calculate expectation values of observables for the classical ensemble by an integral over the phase space

$$\langle O_{x,p} \rangle (t) = \iint w(x, p, t) O(x, p) dp dx \quad (25)$$

likewise for a quantum system by (20). The evolution of $w(x, p, t)$ is determined by the (classical) Liouville equation^{27,28}

$$\frac{\partial w(x, p, t)}{\partial t} = \frac{\partial H(x, p, t)}{\partial p} \frac{\partial w(x, p, t)}{\partial x} - \frac{\partial H(x, p, t)}{\partial x} \frac{\partial w(x, p, t)}{\partial p}, \quad (26)$$

where $H(x, p, t)$ denotes the Hamilton function that also governs the motion of the ensemble's single particles. The equation (26) may be written as a continuity equation (16) by introducing the probability flow

$$\mathbf{j}(x, p, t) = \begin{pmatrix} \frac{p}{m} w(x, p, t) \\ -\frac{\partial V(x, t)}{\partial x} w(x, p, t) \end{pmatrix}. \quad (27)$$

The quantum Liouville equation (14) reduces in the limit $\hbar \rightarrow 0$ to the classical Liouville equation (26). Note, however, that also if the third spatial derivative of the potential $V(x, t)$ and all its higher derivatives vanish the quantum Liouville equation (14) also reduces to the classical Liouville equation (26). This means that the quantum mechanical evolution of the Wigner function for a particle in a homogeneous constant potential or in a harmonic oscillator (or a combination of both) follows the same dynamical law as the probability density of an ensemble of classical particles in the same potential. Nevertheless, non-classical features may be present in the Wigner function.

In summary, quantum theory in phase space in terms of the Wigner function features formal parallels to the classical theory for an ensemble of classical non-interacting particles. The state of both kinds of systems is completely characterized by a real-valued phase space distribution function $w(x, p, t)$. The evolution of $w(x, p, t)$ is determined by the classical Liouville equation (26) or the quantum Liouville equation (14), respectively. The quantum Liouville equation equals its classical counterpart plus some additional quantum terms. For classical systems, $w(x, p, t)$ may be any non-negative normalizable function. The quantum mechanical Wigner function, however, has to be compatible with the laws of quantum mechanics, e. g., to respect the uncertainty relation, and may be negative. Thus, proper quantum characteristics of a quantum dynamical process are governed the additional terms in the quantum Liouville equation or the negative parts of the Wigner function. In fact, the negative parts of the Wigner function are a common measure for non-classicality^{14,16,29,30}.

4. Visualizing quantum dynamics in phase space

After our short review of the Wigner-function's properties in the previous section, we are now prepared to visualize quantum mechanics in phase space. This may be accomplished by picturing the Wigner function itself or quantities that are derived from the Wigner function, e. g., the Wigner function flow (17).

In contrast to the wave function, the Wigner function is a real-valued quantity. It assigns just a single real value to each point in phase space, which simplifies the visualization of Wigner functions to some degree as compared to the visualization of wave functions, which assign two real values to each point in configuration space. The dimension of the phase space—which is twice the configuration-space's dimension—turns out to be a limiting factor when visualizing Wigner func-

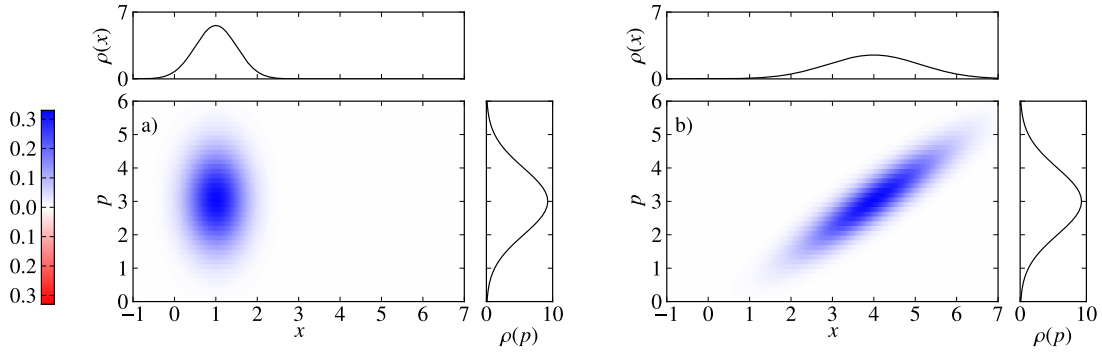


FIG. 2: (Color online) Visualization of the Wigner function (28) of a Gaussian wave packet by false color plots at time $t = 0$ (left part) and $t = 1$ (right part) with $\bar{x} = 1$, $\bar{p} = 3$, and $\sigma = 1/2$ (dimensionless units with $\hbar = 1$ and $m = 1$). The panels above the false color plots show the probability distribution in position space (7a) while panels right next to the false color plots show the probability distribution in momentum space (7b). Values of the Wigner function are indicated by the color-bar at the left.

tions. Therefore, we restrict ourselves in this contribution to systems with a two-dimensional phase space. Displaying two-dimensional real-valued functions is a standard task of scientific visualization and may be accomplished by various methods, e. g., by two-dimensional false color plots (sometimes called heat maps), by contour line maps, which show lines of constant values of the Wigner function, or by (pseudo) three-dimensional surface plots.

Systems with two or more spatial dimensions have a phase space with at least four dimensions which prohibits visualizing the full Wigner function. In this case one may in order to reduce the dimensionality, for example, picture lower dimensional cuts of the Wigner function through the phase space or projections of the Wigner function onto lower dimensional surfaces.

4.1. A free wave packet

The Wigner function of the Gaussian wave packet (2) is given by the strictly positive bivariate normal distribution

$$w(x, p, t) = \frac{1}{\pi\hbar} \exp\left(-\frac{(x - pt/m - \bar{x})^2}{2\sigma^2} - \frac{2\sigma^2(p - \bar{p})^2}{\hbar}\right), \quad (28)$$

which is illustrated in Fig. 2 by two false color plots for two different points in time, for $t = 0$ in part a and for $t = 1$ in part b, respectively. At time $t = 0$, the Wigner function of the Gaussian wave packet is symmetric in phase space with symmetry axes parallel to the x -axis and the p -axis. During the evolution of the wave packet, the Wigner function gets rotated and stretched along the x -axis in phase space. This corresponds to the familiar wave packet broadening in position space, see also the probability distribution in position space (7a) as shown above the false color plots in Fig. 2.

As we pointed out in section 3.2, the quantum Liouville equation (14) of a free quantum particle's Wigner function reduced to the classical Liouville equation (26) for an ensemble of free non-interaction particles with the Hamiltonian

$H(x, p, t) = p^2/(2m)$. Thus, the Wigner function of a free particle satisfies the relation

$$w(x, p, t) = w(x - pt/m, p, 0). \quad (29)$$

As a consequence of (29), we find the equation

$$\rho(x, t) = \int w(x, p, t) dp = \int w(x - pt/m, p, 0) dp, \quad (30)$$

which states that the probability distribution in position space $\rho(x, t)$ at position x and time t is given by an integral over the Wigner function at time zero along phase space strips which are rotated against the p -axis by an angle of $-\arctan t/m$. Thus, measuring the distribution $\rho(x, t)$ of a function of the position x and the time t allows to reconstruct the full Wigner function $w(x, p, 0)$ at time zero by means of an inverse Radon transformation^{11,31}. This has also been demonstrated experimentally¹³⁻¹⁷.

4.2. Characterizing eigen-states

The Wigner function eigen-state of some time independent potential $V(x)$ is determined by the two equations (23a) and (23b). For the harmonic oscillator potential $V(x) = m\omega^2 x^2/2$ we find^{9,11} the eigen-states

$$w_n(x, p) = \frac{(-1)^n}{\pi\hbar} \exp\left(-\frac{p^2}{(\hbar\kappa)^2} - (x\kappa)^2\right) L_n\left(2\frac{p^2}{(\hbar\kappa)^2} + 2(x\kappa)^2\right), \quad (31a)$$

and eigen-energies

$$E_n = \hbar\omega\left(n + \frac{1}{2}\right) \quad (31b)$$

with $\kappa = \sqrt{m\omega/\hbar}$, $n = 0, 1, \dots$ and $L_n(x)$ denoting the n th Laguerre polynomial.

In Fig. 3 we depict the Wigner function of the harmonic oscillator eigen-state with energy $E = \hbar\omega(3 + 1/2)$ together

with its Wigner function flow (17). Because the n th Laguerre polynomial has n positive roots, the Wigner function of the harmonic oscillator eigen-state oscillates and changes n times its sign. Note that despite the fact that the Wigner function (31a) is time-independent there is a permanent circular steady Wigner function flow in phase space as indicated by the arrows in Fig. 3.

In section 3 we demonstrated that for harmonic potentials quantum *dynamical* effects are absent. This means, the dynamics of the Wigner function follows the classical Liouville equation because all quantum terms in the quantum Liouville equation vanish for harmonic potentials. Also in equation (23) quantum terms vanish, which has consequences for the geometry of the Wigner function flow of the eigen-states of the harmonic oscillator. Using equations (17) and (23a) one can show that $\mathbf{j}(x, p) \cdot \nabla w(x, p) = 0$ and, therefore, the Wigner function flow is always tangential to the lines of constant Wigner function values. This is a feature that the harmonic oscillator eigen-states share with all time-independent classical phase space distributions. Also for classical distributions the flow (27) is tangential to the lines of constant phase space distribution.

If the potential has non-quadratic terms then the quantum terms in (23) will affect the structure of the Wigner eigen-functions and the Wigner function flow and the lines of constant Wigner function values are no longer tangential to each other. Thus, the divergence between the direction of the Wigner function flow and the tangentials to the lines of constant Wigner function values may be interpreted as a measure how strong the non-classical terms in the quantum Liouville equation (14) affect the structure of the eigen-states.

In Fig. 4 we show the Wigner function ground states of the anharmonic oscillator potential $V(x) = m\omega^2 x^2/2 + \alpha x^4$ for various values of the anharmonicity parameter α . For this figure

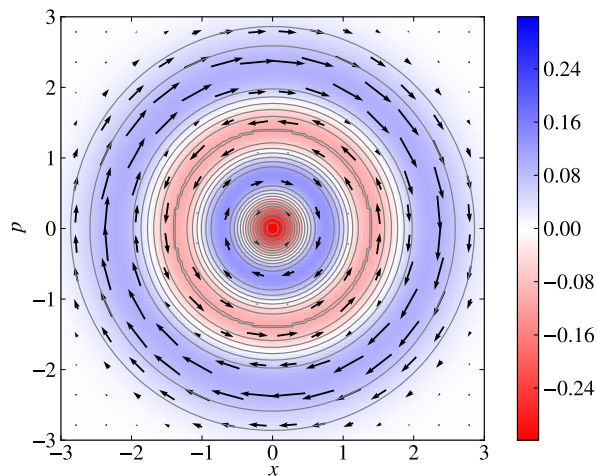


FIG. 3: (Color online) False color plot of the Wigner function of the harmonic oscillator eigen-function with energy $E = 3 + 1/2$ (dimensionless units with $\hbar = 1$, $m = 1$, and $\omega = 1$). Gray solid lines indicate levels of constant Wigner function values while black arrows indicate the steady Wigner function flow (17). The arrows' length is proportional to the flow's magnitude.

the Schrödinger ground state wave functions have been calculated by imaginary time propagation^{32,33} and the Wigner function was obtained by calculating (3) numerically afterward. In Fig. 4 the anharmonicity parameter α grows from left to right starting with $\alpha = 0$ (part a) and increasing to $\alpha = 1/4$ (part b) and $\alpha = 3/4$ (part c). One clearly sees in Fig. 4 how the divergence between the direction of the Wigner function flow and the tangentials to the lines of constant Wigner function values grows with increasing α .

4.3. Scattering by a potential barrier

Scattering of a wave packet by a potential barrier is a well known textbook system to exemplify quantum effects. Depending on the potential's shape and the initial condition of the wave packet some part of the wave packet may be reflected while the other part is transmitted; a process that has no analog in classical physics of point-like particles.

The quantum dynamical scattering dynamics is commonly visualized by the wave function in position space^{4,5} and sometimes in momentum space⁶. Figure 5 illustrates scattering of an initial Gaussian wave packet by a potential barrier in phase space at different points in time. The scattering potential barrier is located around $x = 0$ and its shape is given by

$$V(x) = V_0 \left(\tanh\left(\frac{x}{\Delta}\right) + 1 \right) \left(\tanh\left(-\frac{x}{\Delta}\right) + 1 \right), \quad (32)$$

see also Fig. 5 d. For this figure the Schrödinger wave functions was propagated by a Fourier split operator method³⁴ and the Wigner function was obtained by calculating (3) numerically afterward.

The system in Fig. 5 starts at time $t = 0$ (Fig. 5 a) with an asymptotically free Gaussian wave packet. Here we consider a thin potential with height $V_0 = 64$ and characteristic width $\Delta = 1/8$. The wave packet's initial kinetic energy equals $E_{\text{kin}} = 32$. Accordingly to the laws of classical physics the kinetic energy is too small to cross the barrier. As the wave packet moves towards the potential barrier it starts to interact with the barrier. Due to the non-classical terms of the quantum Liouville equation the Wigner function starts to develop regions with negative values such that at about $t = 1/2$ significant interference patterns have emerged, see Fig. 5 b. At about $t = 1$ the wave packet has split into two parts that are traveling into opposite directions in position space, a reflected part and a transmitted part that has tunneled through the potential barrier. In phase space this corresponds to two isolated wave packets with approximately Gaussian shape moving into opposite directions, see also Fig. 5 c. However, there is also a region with non-zero Wigner function between these two packets that exhibits strong oscillations featuring positive and negative values revealing the quantum nature of the coherent superposition of the two wave packets^{14,17}.

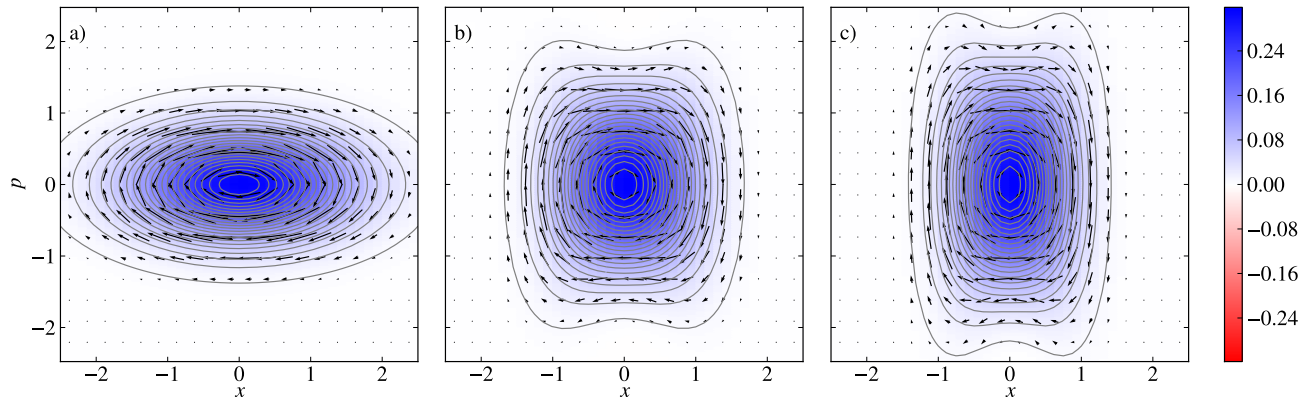


FIG. 4: (Color online) Wigner function ground state of the anharmonic oscillator potential $V(x) = m\omega^2 x^2/2 + \alpha x^4$ for various values of the anharmonicity parameter α with $\alpha = 0$ (part a), $\alpha = 1/4$ (part b), $\alpha = 3/4$ (part c) (dimensionless units with $\hbar = 1$, $m = 1$, and $\omega = 1/2$).

5. Conclusions

In this contribution we have explored ways to visualize quantum mechanics in phase space by means of the Wigner function and the Wigner function flow. The mathematical formalism of quantum mechanics in phase space in terms of the Wigner function resembles classical Hamiltonian mechanics of non-interacting classical particles. Thus, teaching quantum mechanics in phase space may have some advantages when moving from classical to quantum physics. Non-classical features are highlighted in phase space, for example by negative values of the phase space distribution or the divergence between the direction of the Wigner function flow and tangentials to the lines of constant Wigner function values of eigenstates.

Acknowledgments

N. R. I. would like to express her appreciation to the organizers of the XVth International Summer Science School of the city of Heidelberg and to the Max-Planck-Institut für Kernphysik for its hospitality.

¹B. Thaller, *Visual Quantum Mechanics* (Springer, 2000).

²B. Thaller, *Advanced Visual Quantum Mechanics* (Springer, 2000).

³R. Robinett, *Quantum Mechanics: Classical Results, Modern Systems, and Visualized Examples*, 2nd ed. (Oxford University Press, 2006).

⁴S. Brandt and H. D. Dahmen, *The Picture Book of Quantum Mechanics*, 3rd ed. (Springer, 2001).

⁵A. Goldberg, H. M. Schey, and J. L. Schwartz, *American Journal of Physics* **35**, 177 (1967).

⁶A. Goldberg, H. M. Schey, and J. L. Schwartz, *American Journal of Physics* **36**, 454 (1968).

⁷R. P. Feynman, *QED: The Strange Theory of Light and Matter* (Princeton University Press, 1986).

⁸E. Wigner, *Physical Review* **40**, 749 (1932).

⁹M. Hillery, R. F. O'Connell, M. O. Scully, and E. P. Wigner, *Physics Reports* **106**, 121 (1984).

¹⁰C. K. Zachos, D. B. Fairlie, and T. L. Curtright, eds., *Quantum Mechanics in Phase Space: An Overview with Selected Papers* (World Scientific, 2005).

¹¹W. P. Schleich, *Quantum optics in phase space* (Wiley-VCH, 2001).

¹²S. Habib, K. Shizume, and W. H. Zurek, *Physical Review Letters* **80**, 4361 (1998).

¹³D. T. Smithey, M. Beck, and M. G. R. A. Faridani, *Physical Review Letters* **70**, 1244 (1993).

¹⁴C. Kurtsiefer, T. Pfau, and J. Mlynek, *Nature* **386**, 150 (1997).

¹⁵G. Breitenbach, S. Schiller, and J. Mlynek, *Nature* **387**, 471 (1997).

¹⁶A. I. Lvovsky, H. Hansen, T. Aichele, O. Benson, J. Mlynek, and S. Schiller, *Physical Review Letters* **87**, 050402 (2001).

¹⁷S. Deléglise, I. Dotsenko, C. Sayrin, J. Bernu, M. Brune, J.-M. Raimond, and S. Haroche, *Nature* **445**, 510 (2008).

¹⁸I. Bialynicki-Birula, P. Górnicki, and J. Rafelski, *Physical Review D* **44**, 1825 (1991).

¹⁹G. R. Shin, I. Bialynicki-Birula, and J. Rafelski, *Physical Review A* **46**, 645 (1992).

²⁰S. Varró and J. Javanainen, *Journal of Optics B: Quantum and Semiclassical Optics* **5**, S402 (2003).

²¹C. H. Keitel, *Contemporary Physics* **42**, 353 (2001).

²²O. T. Serimaa, J. Javanainen, and S. Varró, *Physical Review A* **33**, 2913 (1986).

²³R. L. Hudson, *Reports on Mathematical Physics* **6**, 249 (1974).

²⁴J. E. Moyal, *Mathematical Proceedings of the Cambridge Philosophical Society* **45**, 99 (1949).

²⁵A. Peres, *Quantum Theory: Concepts and Methods* (Kluwer Academic Publishers, 1993).

²⁶We do not distinguish in our notation between the Wigner function and the classical probability distribution. It should be clear from the context whenever $w(x, p, t)$ denotes a Wigner function or a classical probability distribution.

²⁷P. Gaspard, *Chaos, Scattering and Statistical Mechanics*, Cambridge Non-linear Science Series, Vol. 9 (Cambridge University Press, 1998).

²⁸F. Schwabl, *Statistical mechanics*, Advanced texts in physics (Springer, 2006).

²⁹A. Kenfack and K. Życzkowski, *Journal of Optics B: Quantum and Semiclassical Optics* **6**, 396 (2004).

³⁰M. Mahmoudi, Y. I. Salamin, and C. H. Keitel, *Physical Review A* **72**, 033402 (2005).

³¹D. Leibfried, T. Pfau, and C. Monroe, *Physics Today* **51**, 22 (1998).

³²A. Goldberg and J. L. Schwartz, *Journal of Computational Physics* **1**, 433 (1967).

³³A. Goldberg and J. L. Schwartz, *Journal of Computational Physics* **1**, 448 (1967).

³⁴M. D. Feit, J. A. Fleck, Jr., and A. Steiger, *Journal of Computational Physics* **47**, 412 (1982).

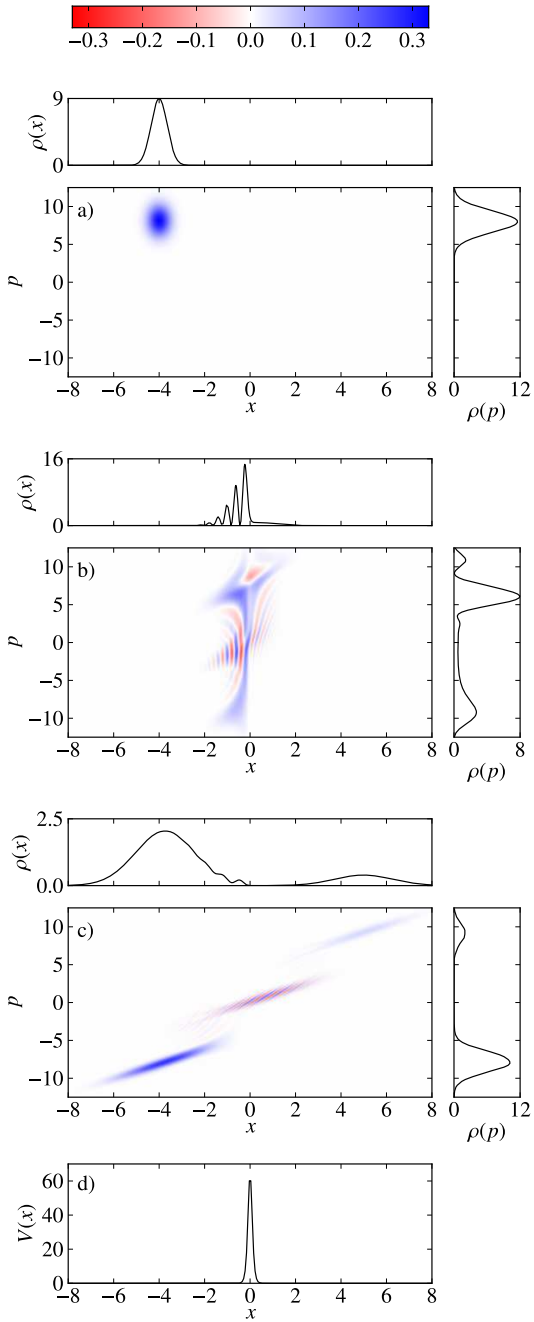


FIG. 5: (Color online) Scattering of a wave packet by a potential barrier (32) in phase space. Potential parameters are $V_0 = 64$ and $\Delta = 1/8$, the wave-packet's initial mean momentum is 8, all values in dimensionless units with $\hbar = 1$ and $m = 1$. The three upper panels show the Wigner function, the position space probability distribution and the momentum space probability distribution at different times; $t = 0$ (part a), $t = 1/2$ (part b), and $t = 1$ (part c). Part d illustrates the scattering potential (32).